Chimia 55 (2001) 497–504

ISSN 0009–4293

Solving Complex Zeolite Structures from Powder Diffraction Data

Lynne B. McCusker*, Christian Baerlocher, Ralf Grosse-Kunstleve, Simon Brenner, and Thomas Wessels

Abstract: To understand the technologically important properties of zeolites and their analogs, structure analysis is essential. However, most new zeolites are prepared in polycrystalline form, so powder diffraction methods of structure solution must be applied, and these have their limitations. In an effort to extend the range of structural complexity that can be addressed when only powder diffraction data are available, a number of new approaches have been explored in recent years. Three that were developed in our research group are described. The first involves the active use of chemical information in an automated structure solution process (*focus*); the second, the generation of structure envelopes to facilitate structure solution in direct (model-building) space; and the third, the exploitation of preferred orientation (texture) to obtain better estimates of the relative intensities of overlapping reflections. The *focus* approach is specific to zeolites, but the other two are generally applicable. All three methods have been applied to real problems, and examples are given. The determination of the structure of the high-silica zeolite UTD-1F, with 117 atoms in the asymmetric unit, using the texture approach demonstrates the power of powder diffraction techniques in structure analysis.

Keywords: FOCUS · Powder diffraction · Structure envelope · Texture · Zeolite structure determination

1. Introduction

1.1. *Zeolites*

Zeolites are key components in a number of industrial processes. They are used as shape-selective acid catalysts in the petrochemical industry, as water softeners in laundry detergents, as desiccants in the laboratory (or *e.g.* between the panes of glass in double-glazed windows), as concentrators of isotopes in the treatment of radioactive waste, and even as additives in animal feeds. More recently, they have also been shown to be suitable as hosts for periodic nanometer-scale arrangements of active centers in nanotechnological materials. Despite the apparent diversity of the listed applications, there is a common denominator: the unusual structures of these crystalline microporous materials.

Classically, zeolites are defined as aluminosilicates with open three-dimensional framework structures composed of corner-sharing tetrahedra. As an example, the framework structure of the mineral faujasite (**FAU** framework type) is shown in Fig. 1. Its synthetic analog, zeolite Y, is the prime catalyst in oil cracking and reforming processes. Cations that balance the charge of the anionic framework are loosely associated with the framework oxygens, and the remaining pore volume is filled with water molecules. The cations are labile and can be exchanged with other cations (including protons) relatively easily, and the water can be removed by simple heating without a collapse of the framework structure or its pore system. Thus, zeolites are excellent ion-exchangers, and, in the dehydrated form, adsorbents. The original definition has now been expanded to include tetrahedrally coordinated elements other than Si and Al in the framework, and organic species in the pores. As of December 2000, there were 133 confirmed zeolite framework types [1]. The key feature of any zeolite is its periodic pore system with channels and cavities of well-defined size and shape. The nature of the pore system (*i.e.* its dimensionality, the size of the pore openings, the size of the cavities, the number and type of extra-framework cation sites, and the spacing between cages) is the dominant factor that will determine a particular zeolite's suitability for a given application. Thus, to understand zeolite chemistry, structure analysis is essential.

Unfortunately, new synthetic zeolites often materialize in the form of polycrystalline powders, and even concerted efforts to make single crystals tend to be unsuccessful. This means that structure analysis cannot be performed using standard crystallographic techniques, so for us the development of methods for determining their structures from powder diffraction data is an integral part of zeolite structure analysis.

1.2. *Powder Diffraction*

An 'ideal' polycrystalline sample contains literally millions of tiny crystallites arranged in all possible orientations. In an X-ray diffraction experiment, each of these crystallites generates its own single-crystal diffraction pattern (each with its own orientation), and the result is shown in Fig. 2. For simplicity, a two-

*Correspondence: Dr. L.B. McCusker
Laboratory of Crystallography
ETH-Zentrum
CH-8092 Zürich
Tel.: +41 1 632 3721
Fax: +41 1 632 1133
E-Mail: mccusker@kristall.erdw.ethz.ch
http://www.kristall.ethz.ch/~lynne/

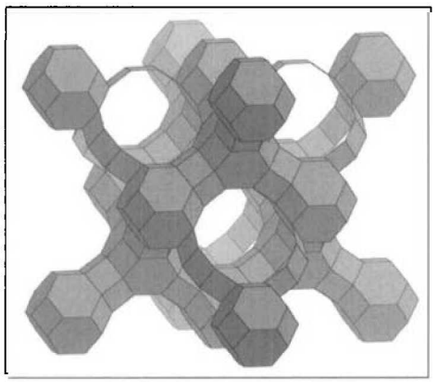

Fig. 1. The framework structure of the mineral faujasite (**FAU** framework type). Each node represents a Si or Al atom. The oxygen bridges between these atoms have been omitted for clarity. Rings with six or fewer Si or Al atoms have been made opaque to highlight the large 12-ring channels.

dimensional case is illustrated, but extrapolation to three dimensions is straightforward. For the single crystal (Fig. 2a), all reflections are well-separated in space, and their individual intensities can be measured easily. For the 'ideal' powder (Fig. 2b), the diffraction pattern is simply a superposition of millions of differently oriented single-crystal diffraction patterns. As a result, reflections with similar *d*-spacings overlap in space and only the sum of their intensities can be measured. For example, the three reflections highlighted in the single-crystal pattern fall on top of one another in the 'ideal' powder diffraction pattern, so their individual intensities cannot be determined.

In principle, a powder diffraction pattern contains all the information present in a single-crystal diffraction pattern, but because of this overlap, some of that information is obscured. If the degree of overlap is low, single-crystal structure determination techniques can often be applied to the powder diffraction data quite successfully, but if it is high, there is usually too much ambiguity in the reflection intensities to allow standard crystallographic methods to function properly.

The degree of overlap is a function of the geometry of the unit cell, the instrument used to collect the data, and the sample itself. For cubic, tetragonal and hexagonal crystal systems, some reflections will automatically overlap exactly (*e.g.* in the cubic case, the 333 and 511 reflections have identical *d*-spacings). The likelihood of accidental reflection overlap (*i.e.* not dictated by the symmetry) increases (1) with the size of the unit cell (density of reflections increases), (2) if one of the unit cell dimensions is by chance similar to another (e.g. $a \sim b$ or $a \sim 2b$), and (3) with increasing 2θ. Obviously, the degree of overlap is also a function of how sharp the reflections are, and this in turn is a function of the crystalline quality of the sample and the instrument used to perform the measurement.

For the *refinement* of a structure, the problem of reflection overlap in a powder diffraction pattern can be circumvented by using the Rietveld method [2]. In this whole-profile approach, the intensities of the observed and calculated patterns are compared on a point by point rather than a reflection by reflection basis, so the intensities of the individual reflections under a single peak of the diffraction pattern do not have to be known explicitly. The method only requires that profile parameters to describe the shapes of the peaks in the pattern be refined in addition to the structural parameters. The method has proven to be an extremely powerful one, and some very complex structures have been refined using it [3][4]. Of course, refinement implies that a starting structural model is available. If this is not the case, the problem becomes more difficult.

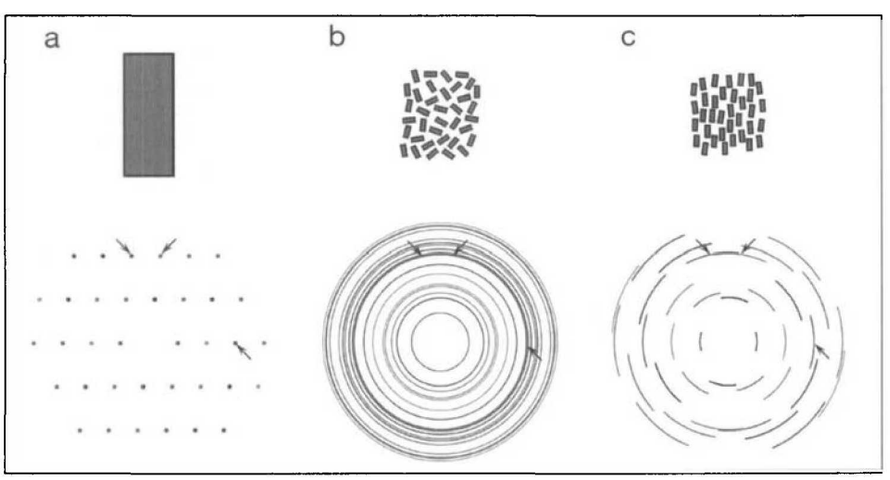

Fig. 2. Schematic drawings of a sample and its corresponding diffraction pattern for (a) a single crystal, (b) a powder with randomly oriented crystallites, and (c) a textured powder. The arrows highlight three reflections with similar diffraction angles that are separated in the single-crystal pattern, but overlap in the normal powder pattern. The diffraction angle increases radially from the center of each diffraction pattern.

1.3. *Solving Structures from Powder Diffraction Data*

If an approximate structure is not known in advance, a whole-profile refinement without a structural model can be performed to extract a set of reflection intensities from the powder diffraction pattern. In this case, the intensities of the reflections rather than structural parameters are refined to obtain the best fit between the observed and calculated patterns [5][6]. Obviously, the intensities of overlapping reflections are highly correlated, and cannot be determined separately. For convenience, the intensity of a composite peak in the diffraction pattern is usually divided equally (equipartitioned) over the contributing reflections. This set of data then resembles a single-crystal dataset and can be used as input to standard crystallographic programs. However, if there are too many ambiguities in the intensities (*i.e.* too much reflection overlap), this approach to structure solution is unlikely to work.

To improve the chances of success, three different philosophies have been followed by various research groups. One is to try to improve the estimate of the relative intensities of overlapping reflections to obtain a more single-crystal-like dataset, the second is to adapt single-crystal methods to address the problems inherent to powder diffraction data, and the third is to incorporate chemical knowledge into the structure solution process. For further details, the reader is referred to the book *Structure Determination from Powder Diffraction Data* edited by David *et al.* [7].

1.4. *Approaches Developed in Our Research Group*

Our research group at the ETH in Zürich has a long-standing interest in zeolite structure analysis, and thereby in powder diffraction methodology. In recent years, we have been concentrating on the problem of zeolite structure determination from powder diffraction data, and have developed three very different approaches. One involves the active use

of chemical information in an automated structure solution process, the second the generation of structure envelopes to facilitate structure solution in direct (model-building) space, and the third the exploitation of preferred orientation (texture) to obtain better estimates of the relative intensities of overlapping reflections. Each of these will be discussed in turn in the following sections.

2. Using Chemical Information in the Structure Solution Process

The classical approach to solving the structure of a polycrystalline material is to build a physical model that is consistent with all of the information known about the compound. This model is then used to calculate a powder diffraction pattern for comparison with the measured one. Although model building is a very powerful technique, because it takes all information (*i.e.* not just the diffraction data) into account, it is extremely inefficient, uncomfortably dependent upon the experience and ingenuity of the model builder, and depressingly prone to failure. Nonetheless, it is often the only option available for complex structures, and the zeolite structure literature is rich in impressive examples of successful model building.

While it is perhaps difficult to convert the intuitive thought processes and all the knowledge of an experienced model builder into the strict logic of a computer program, some quantifiable characteristics (*e.g.* chemical composition, expected coordination geometries, and typical bond distances and angles) would seem to lend themselves to a computer-aided approach. Thus, a way of including such information in an automated structure solution procedure was sought. The intuition would be replaced with pure computing power that allows thousands or even millions of trial structures to be generated and evaluated.

2.1. *The Computer Program* focus

The result of these efforts was the computer program *focus* [8]. In addition to computing power, the program exploits the fact that a zeolite's chemical composition, its approximate density, its unit cell dimensions, and typical interatomic distances for its framework atoms are generally known, and that the most likely space group(s) can usually be deduced. The key to the program lies in its active use of the information that a zeolite always has a three-dimensional, four-connected framework structure. The flow chart in Fig. 3 delineates the logic of the program.

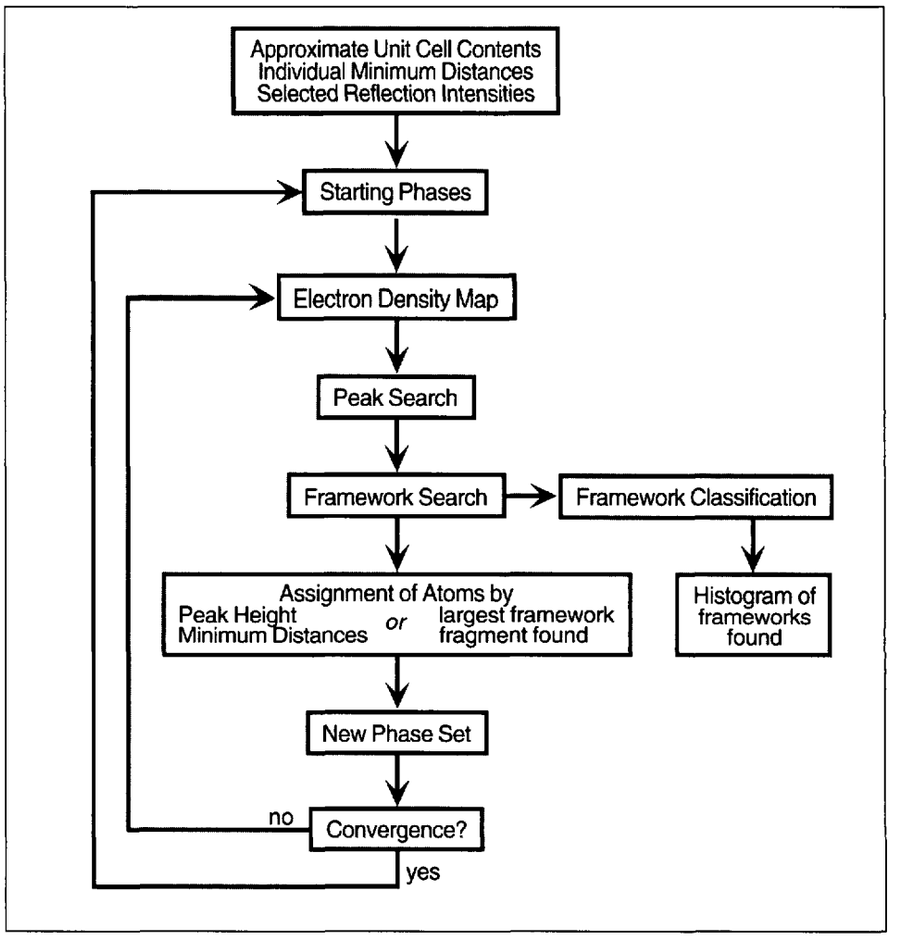

Fig. 3. Flow chart for the zeolite structure determination program *focus*.

The input consists of a set of reflection intensities extracted from the powder diffraction pattern, the unit cell, the (assumed) space group, the number and type (*e.g.* node or bridge) of framework atoms in the unit cell, and the minimum distances expected between the different framework atoms. Random phases consistent with the restrictions of the space group are assigned to the reflections, and an electron density map is generated. An attempt is then made to interpret this (possibly nonsensical) electron density map using the chemical information given. This is done in one of two ways. The peaks in the map are assigned either (1) in a traditional way according to their height in view of the chemical composition of the material, but taking the minimum interatomic distances into account, or (2) according to the largest framework fragment found. For the latter, peak height is given a lower priority. Once the map has been interpreted, the resulting model is used to calculate new phases for the reflections and a new electron density map is generated. This Fourier recycling is continued until the phases have converged or a prescribed maximum number of cycles has been reached. No matter how the electron density map is interpreted, each time one is generated, an exhaustive search for a three-dimensional four-connected framework structure with appropriate interatomic distances is conducted. If such a framework is found, it is written to a file. When the Fourier recycling loop is completed, the process is continued with a new set of random phases.

The frameworks found are classified (a unique framework topology can be recognized by the coordination sequences and loop configurations of its node atoms [1]), and the process can be stopped when one framework clearly dominates over others. The rationale of the program is that if enough of the phases are (by chance) correct, some features of the structure will appear (though perhaps weakly) in the electron density map, and the Fourier recycling process will reinforce the correct features until the full structure can be recognized. Different starting phase sets will reveal different

features initially, but if the features are correct, the Fourier recycling process should eventually produce the full structure. Thus the correct framework will be found from many different starting points, and will therefore be found most often.

2.2. *SSZ-44*

A list of zeolite structures that have been solved using *focus* is given in the Table. Some of these are test structures used during the development of the program (ref. *a)* in the Table), but the others are real structure solutions. One of the more complex of the latter, the high-silica zeolite SSZ-44 solved by a non-Zürich group [9], is given here as an example. Reflection intensities were extracted from synchrotron powder diffraction data out to a *d*-value of 1.3 Å (overlapping reflections equipartitioned), and used as input to *focus* along with the space group and the lattice parameters ($P2_1/m$, a = 11.485 Å, b = 21.946 Å, c = 7.388 Å, β = 94.7°, V = 1856 Å^3). The result was the framework structure (with 8 Si and 17 O in the asymmetric unit) shown in Fig. 4. This structure could then be used to elucidate that of a related zeolite SSZ-35, which had exhibited similar catalytic activity. The layers related by mirror planes in SSZ-44 are related by inversion centers in SSZ-35.

Table. Zeolite structures determined using *focus*

Material	Framework Composition	Space Group	T-atoms / asym. unit	Framework Type Code
NU-3 [a]	$[Si_{54}O_{108}]$	$R\bar{3}m$	2	LEV
Zeolite A [a]	$[Al_{96}Si_{96}O_{384}]$	$Fm\bar{3}c$	2	LTA
MCM-61 [b]	$[Si_{28}Al_2O_{60}]$	$R\bar{3}m$	3	MSO
SAPO-40 [a]	$[(Si,Al,P)_{32}O_{64}]$	$Pmmn$	4	AFR
EMC-2 [a]	$[(Si,Al)_{96}O_{192}]$	$P6_3/mmc$	4	EMT
Dodecasil-1H [a]	$[Si_{34}O_{68}]$	$P6/mmm$	4	DOH
GUS-1 [c]	$[Si_{32}O_{64}]$	$C222$	4	GON
CIT-5 [d]	$[Si_{32}O_{64}]$	$Pmn2_1$	5	CFI
Cloverite [a]	$[(Ga,P)_{768}O_{1488}(OH)_{96}]$	$Pm\bar{3}m$	5	-CLO
ICR-1 [e]	$[Si_{44}O_{88}]$	$C2/m$	6	MTF
YUL-86 [f]	$[Al_{12}P_{12}O_{48}]$	$P2_1/c$	6	AWO
$AlPO_4$-53(C) [g]	$[Al_{24}P_{24}O_{96}]$	$C2$	6	AEN
VPI-9 [h]	$[Si_{48}Zn_{12}O_{120}]$	$P4_2/ncm$	7	VNI
YUL-90 [f]	$[Al_{32}P_{32}O_{128}]$	$Pbca$	8	ZON
SSZ-44 [i]	$[Si_{32}O_{64}]$	$P2_1/m$	8	SFF
RUB-17 [a]	$[Si_{28}Zn_8O_{72}]$	Cm	9	RSN
ZSM-5 [a]	$[Si_{96}O_{192}]$	$Pnma$	12	MFI

a) Test cases used during the development of *focus;* R.W. Grosse-Kunstleve, 'Zeolite Structure Determination from Powder Data: Computer-based Incorporation of Crystal Chemical Information', ETH-Dissertation Nr. 11422, **1996.**
b) D.F. Shantz, A. Burton, R.F. Lobo, *Microporous and Mesoporous Materials* **1999**, *31*, 61.
c) J. Plévert, Y. Kubota, T. Honda, T. Okubo, Y. Sugi, *Chem. Commun.* **2000**, 2363.
d) P. Wagner, CalTech, Pasedena, CA and R.W. Grosse-Kunstleve, Lawrence Berkeley Laboratory, Berkeley, CA, *personal communication.*
e) S. Brenner, ETH, Zürich, *personal communication.*
f) R.W. Grosse-Kunstleve, L.B. McCusker, C. Baerlocher, *J. Appl. Crystallogr.* **1999**, *32*, 536.
g) R.M. Kirchner, R.W. GrosseKunstleve, J.J. Pluth, S.T. Wilson, R.W. Broach, J.V. Smith, *Microporous and Mesoporous Materials* **2000**, *39*, 1387.
h) L.B. McCusker, R.W. Grosse-Kunstleve, C. Baerlocher, M. Yoshikawa, M.E. Davis, *Microporous Materials* **1996**, *6*, 295.
i) P. Wagner, S.I. Zones, M.E. Davis, R.C. Medrud, *Angew. Chem. Int. Ed.* **1999**, *38*, 1269.

3. Structure Envelopes

While *focus* proved to work very well, even for complex zeolite structures, careful testing of the program highlighted its limitations [10]. A complex framework structure like that of ZSM-5, with 12 Si and 26 O in the asymmetric unit, can be solved quite straightforwardly, but the input parameters must be carefully chosen if the computing time is to remain reasonable. An interrupted framework (*i.e.* one that is not fully four-connected), like that of the gallophosphate cloverite, can also be solved, but the ambiguity in the connectivity of the individual tetrahedral atoms leads to a much slower framework search. An average zeolite structure with four to six tetrahedrally coordinated atoms (T-atoms) in the asymmetric unit can be solved in a matter of minutes or hours, but as the complexity/ambiguity increases so does the computing time. To reduce the number of possible solutions for complex structures, and thereby the computing time required, we investigated the possibility of using a structure envelope, similar to the molecular envelope used in protein crystallography, to restrict the framework search to selected regions of the asymmetric unit.

3.1. *Periodic Nodal Surfaces and Structure Envelopes*

In a roundabout way, Brenner *et al.* [11] discovered that a structure envelope can be derived from a density map generated from just a few (usually between one and five) strong, low-order reflections (*i.e.* precisely those that are least likely to be involved in overlap in a powder diffraction pattern) using the equation

$$\rho(x,y,z) = \sum_{hkl} E_{hkl} \cos(2\pi(hx + ky + lz) - \alpha_{hkl}) \qquad (1)$$

where $\rho(x,y,z)$ is the density at point (x,y,z) in the unit cell, E_{hkl} is the normalized structure factor for reflection *hkl* and α_{hkl} is its phase. The points at which the density $\rho(x,y,z)$ is zero (*i.e.* the roots of the equation) describe a periodic nodal surface (PNS) that separates the regions of high electron density from those of low electron density. Because this surface envelops the structure, but does not necessarily have a closed form like a molecular envelope, we dubbed it a 'structure envelope'. As an example, the structure envelope generated for the high-silica zeolite ITQ-1 (**MWW** framework type) from the 002, 100, 101 and 102 reflections is shown in Fig. 5. It is readily apparent that such an envelope could be used to restrict a search routine to the more promising regions of the unit cell.

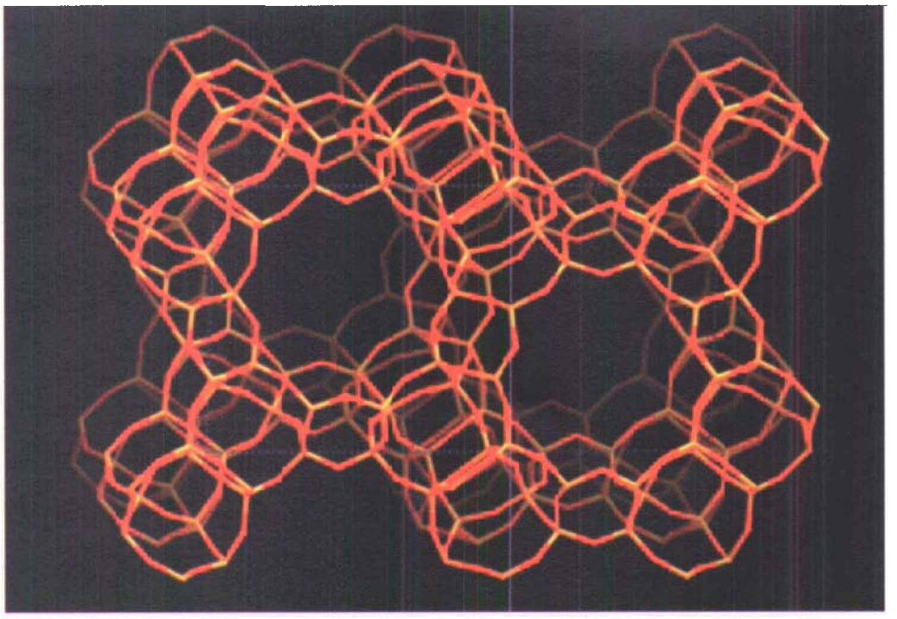

Fig. 4. The framework structure of the high-silica zeolite SSZ-44 (**SFF** framework type) with 8 Si- and 17 O-atoms in the asymmetric unit.

3.2. *Estimating the Phases*

To generate a structure envelope from a powder diffraction pattern, the appropriate reflections must be selected (strong, low-order, all directions in reciprocal space represented) and their phases determined. While the former is a relatively straightforward and non-critical procedure, the latter is not. However, the phases for only a few reflections are required (in some cases origin defining reflections alone suffice, so no phases have to be determined), and an algorithm (*SayPerm*) to estimate these phases has been devised [12]. *SayPerm* is based on the Sayre equation [13] and uses the concept of a pseudo-atom (*e.g.* an SiO_4 tetrahedron is treated as an atom) to simulate atomic resolution at $d = 2.7$ Å (*ca.* 33°2θ for CuKα_1 radiation) and error correcting codes [14] to reduce the number of permutations needed to sample phase space uniformly. This approach has been shown to work very well for zeolite structures, where the contrast in the electron density between the framework and the pores is considerable.

3.3. *Combining a Structure Envelope with* focus

To test the effect of using a structure envelope as a mask in a zeolite structure solution, the framework search routine of *focus* was applied to a simple grid (*ca.* 0.5 Å mesh) within the unit cell, where each point was considered to be a potential atom. Five zeolites with different symmetries and complexities were examined, and the results are given in Fig. 6. It is immediately apparent that the time required to solve the structure without the structure envelope mask increases markedly with the structural complexity (number of T-atoms in the asymmetric unit). In fact, two searches had to be interrupted before the search was complete. With the structure envelope, however, all structures were found in less than 30 min CPU time. This dramatic reduction in computing time by as much as two orders of magnitude can be attributed to the fact that the structure envelope mask not only reduces the volume of the asymmetric unit in which the search is conducted by a factor of approximately two, but its shape also imposes a severe restriction on the number of geometrically feasible solutions.

To test the effect of combining a structure envelope mask with the full power of *focus* (*i.e.* using the powder diffraction data and the Fourier recycling routine as well as the framework search algorithm), the high-silica zeolite ZSM-5, with 12 T-atoms in the asymmetric unit (*Pnma*, $a = 20.063$ Å, $b = 19.938$ Å, $c = 13.409$ Å, $V = 5364$ Å^3), was examined. The five strong reflections 011, 102, 301, 200 and 020 were selected to generate the structure envelope. Three of these reflections are origin-defining, and the phases for the other two were estimated using *SayPerm*. Without the structure envelope mask, *focus* found the framework structure 50 times in 8 h. With the mask, this time could be reduced to 3 h. Weighting the positions from a Fourier map using the structure envelope mask was also found to reduce the computing time when Fourier recycling was applied.

It is clear that the information contained in the structure envelope can be used to advantage in any crystallographic procedure that functions in direct space. Its effectiveness has also been demonstrated in conjunction with a simulated annealing algorithm for organic molecules [12].

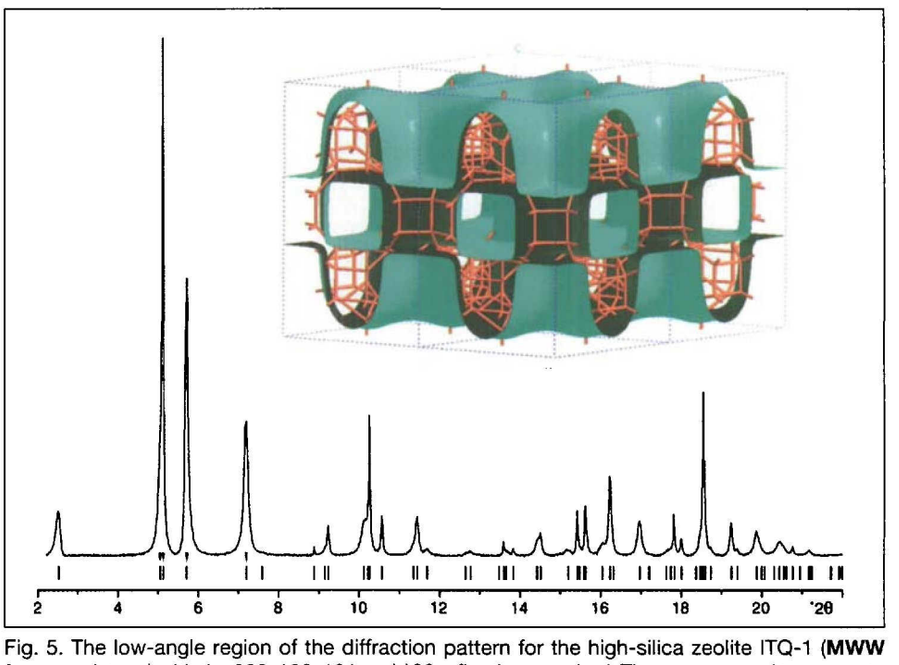

Fig. 5. The low-angle region of the diffraction pattern for the high-silica zeolite ITQ-1 (**MWW** framework type) with the 002, 100, 101 and 102 reflections marked. These were used to generate the structure envelope shown in the inset. Note that the framework Si atoms are all located on the green side of the surface.

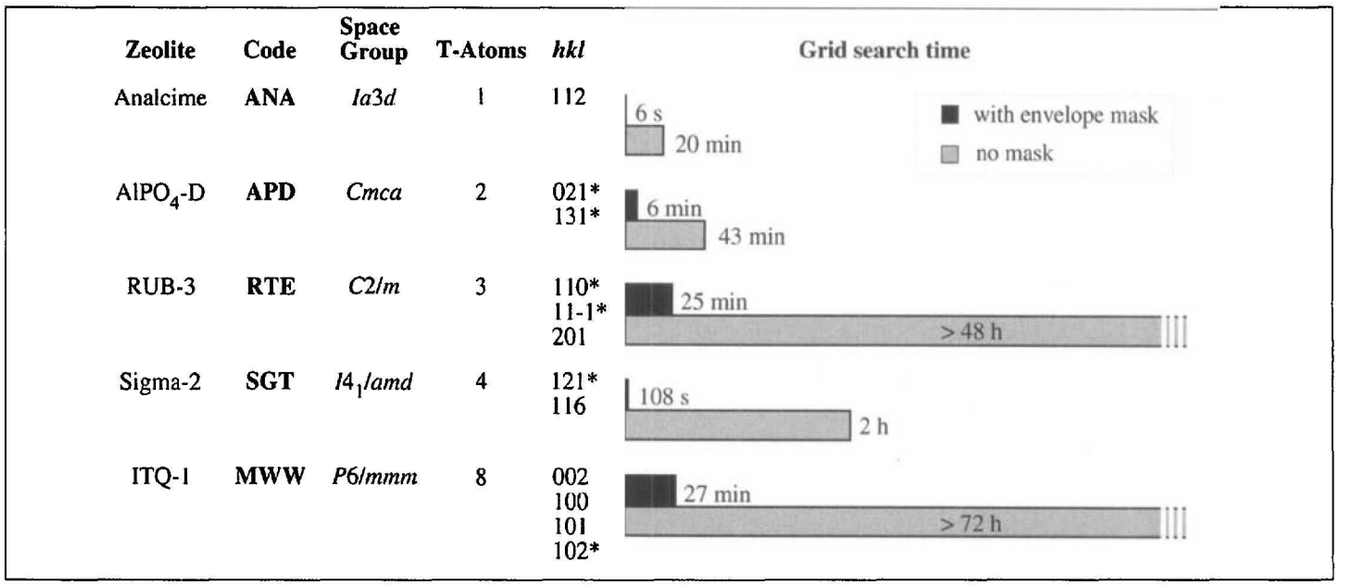

Fig. 6. Grid search times with and without a structure envelope mask. The reflections listed were used to generate the structure envelope. Those marked with an asterisk are origin defining reflections (*i.e.* phase can be assigned arbitrarily).

4. Using Textured Samples to Obtain more Single-crystal-like Data

Since the limitation of powder diffraction data for structure determination lies in the overlap of reflections in 2θ, it is logical to consider ways of improving the estimation of the relative intensities of these overlapping reflections. A more single-crystal-like dataset would allow the very powerful single-crystal methods of structure analysis to be applied. One way of approaching this problem is to adopt a more elaborate data collection strategy in which several different, but related, data sets are collected on the same sample. A sample with a preferred orientation of the crystallites, for example, will yield a diffraction pattern whose intensities are dependent upon the orientation of the sample in the X-ray beam. By collecting data with the sample in several different orientations, more information about the relative intensities of reflections that overlap in 2θ, but not in orientation space, can be gleaned.

Model calculations reported by Hedel and co-workers [15] showed that powder diffraction data from a textured sample (*i.e.* one in which a homogeneous preferred orientation of the crystallites is present or can be induced) can be analyzed to yield a near single-crystal dataset, and indeed Lasocha and Schenk [16] and Cerny [17] have performed experiments along this line using simple descriptions of the texture. It was hoped that by using a more sophisticated experimental set-up and by applying a complete texture analysis to the data, the full power of this approach could be realized [18].

4.1. *Concept*

The idea behind the method can be seen in Fig. 2c, where the diffraction pattern of a textured powder sample is shown together with those for a single crystal and 'ideal' powder. The textured powder sample lies somewhere between these two extremes. The three overlapping reflections in Fig. 2b are separated in 2c. Because not all crystallite orientations are equally represented in the textured sample, the reflections are concentrated in certain regions of reciprocal (diffraction) space, so by measuring the diffraction pattern along different radial directions (*e.g.* by orienting the sample), additional intensity information can be extracted. The appropriate sample orientations, of course, will depend upon the orientations of the crystallites in the sample. Therefore, in order to interpret the measured intensities correctly, the so-called orientation distribution function must be determined.

4.2. *Experimental Setups*

Two experimental setups to collect data from a textured sample have been developed on the Swiss-Norwegian Beamlines (SNBL) at the ESRF in Grenoble: one in *reflection mode* (Fig. 7a, Beamline BM01B) and the other in *transmission mode* (Fig. 7b, Beamline BM01A). In order to orient the sample in the X-ray beam, a controlled way of tilting and rotating the sample is necessary. In *reflection mode*, this is accomplished by attaching two additional circles (χ for the tilt and ϕ for the rotation) to the powder diffractometer, to produce an experimental setup very similar to that of a standard four-circle single-crystal diffractometer. The use of a parallel beam in conjunction with a pre-detector analyzer crystal allows high-resolution data to be collected at all tilt angles. This is in contrast to a typical laboratory setup, where tilting the sample causes a violation of the parafocusing condition so very broad diffraction peaks are obtained at high tilt angles. In *transmission mode*, an area detector is used, so only the rotation axis ϕ is needed for data collection. For data analysis, the individual imaging-plate frames are divided into radial wedges to give the equivalent of a tilt angle (δ).

The *reflection* setup has the advantage that very high resolution powder diffraction patterns can be collected at any tilt angle, but has the disadvantages that a careful calibration of the intensity reduction as a function of tilt and 2θ is needed and that *ca.* 3 days of synchrotron beamtime are required for each sample. Even with this long data collection time, only a few full diffraction patterns can be measured, and the counting statistics for high χ or 2θ angles are not optimal. The *transmission* setup, on the other hand, yields only medium resolution data (dependent upon the size of the sample and the sample-detector distance), but requires only 3–6 h of beamtime per sample. Furthermore, the use of an area detector rather than a point detector allows full diffraction patterns to be collected for *all* sample orientations.

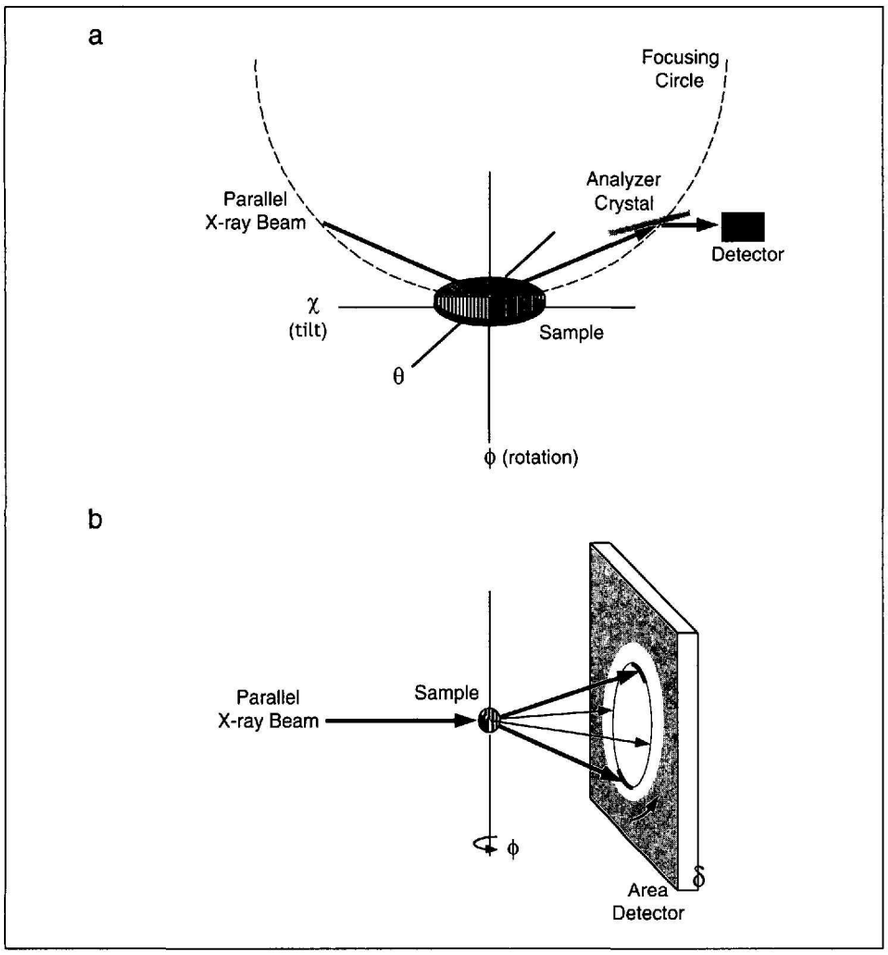

Fig. 7. The two experimental setups for texture measurements (a) in reflection mode and (b) in transmission mode.

4.3. *Data Collection*

To determine how the crystallites are oriented in the sample, pole-figure data (variation in the intensity of a single reflection as a function of sample orientation) for several non-overlapping reflections are required. With the *reflection-mode* setup, appropriate reflections are selected and pole-figure data are collected in steps of 5° in both ϕ and χ (360/5 x 75/5 + 1 = 1081 sample orientations for a maximum tilt angle of 80°). When enough pole figures have been measured, four or five full diffraction patterns are measured at those sample orientations (χ,ϕ) that appear to give the highest intensity differences.

A typical *transmission-mode* dataset consists of 36 imaging plate frames, where each frame corresponds to a 5° rotation of the sample (ϕ). Each frame is divided into 72 (5°) radial wedges (*i.e.* 72 different sample tilts δ), to give a total of 36 frames x 72 wedges = 2592 full diffraction patterns, each corresponding to a different sample orientation (δ,ϕ). Pole-figure data are therefore measured automatically for all reflections.

4.4. *Data Analysis*

In *reflection mode*, data analysis is based on the Eqn.

$$y(2\theta,\chi,\phi) = \sum_{hkl} I_{hkl} P_{hkl}(\chi,\phi) G(2\theta - 2\theta_{hkl}) \quad (2)$$

where y is the intensity of the powder diffraction pattern at step 2θ for sample orientation (χ,ϕ), the summation is over all reflections contributing to the intensity at that step, I_{hkl} is the true integrated intensity of reflection *hkl* (single-crystal value), $P_{hkl}(\chi,\phi)$ is its pole-figure value, which is a measure of how much of the total intensity of reflection *hkl* will be measured at the sample orientation (χ,ϕ), and $G(2\theta\text{-}2\theta_{hkl})$ is the peak profile function. A two-step procedure is used to extract the single-crystal-like intensities I_{hkl}. First, the texture of the sample is determined using one of the standard texture analysis programs, so the values $P_{hkl}(\chi,\phi)$ can be calculated, and then Eqn. (2) is solved for I_{hkl} using all of the measured diffraction patterns. The approach for *transmission* data is very similar (χ in Eqn. (2) is replaced with δ), but involves much more data. More pole figures can be used to determine the texture of the sample, so the values for P_{hkl} are more reliable, and over 2500 powder patterns can be used to determine the values of I_{hkl}.

4.5. *High-silica Zeolite UTD-1F*

As this texture method was being developed (initially in reflection mode), several zeolites of known structure were used as test examples. When these proved to yield reasonable results, some materials of unknown structure were investigated. One of these was a sample of a complex high-silica zeolite UTD-1F ($P2_1/c$, a = 14.963 Å, b = 8.470 Å, c = 30.010 Å, β = 102.7°) provided by Dr. E.J. Creyghton from Shell, Amsterdam.

The needle-like crystallites (*ca.* 0.5 x 0.5 x 40 μm^3) were aligned using shear forces in a polystyrene matrix, and then pole-figure data for seven reflections and full diffraction patterns at five different sample orientations were collected in reflection mode. To illustrate the nature of the data, one of the pole figures and small sections of the diffraction patterns are shown in Fig. 8. A set of intensities was extracted using the procedure described above, and then used as input to a standard direct methods program running in default mode. This resulted in an *E*-map showing the positions of 16 Si- and 17 O-atoms. The Si-atoms described a complete three-dimensional four-connected framework structure with 14-ring pores, and all of the O-atoms were in bridging positions. A difference electron density map then allowed the remaining 15 framework oxygens, and a non-framework cobalt ion to be located.

Then a difference electron density map was generated using this model and high-resolution powder diffraction data collected on an untextured sample of UTD-1F. The map revealed the location of the pentamethylcyclopentadienyl (Cp*) ligands coordinated to the Co ion in the 14-ring channels very clearly. This structure, with a total of 69 atoms (16 Si + 32 O + 1 Co + 20 C) in the asymmetric unit, gave a good initial fit to the diffraction pattern, but the short distances between symmetry-related $Co(Cp^*)_2^+$ complexes required that a disordered model be assumed. Subsequent Rietveld refinement proved to be somewhat unstable and small but significant differences between the observed and calculated diffraction patterns over the full 2θ range were apparent. Consequently, a reduction of the symmetry to *Pc* was attempted, even though the concomitant increase in

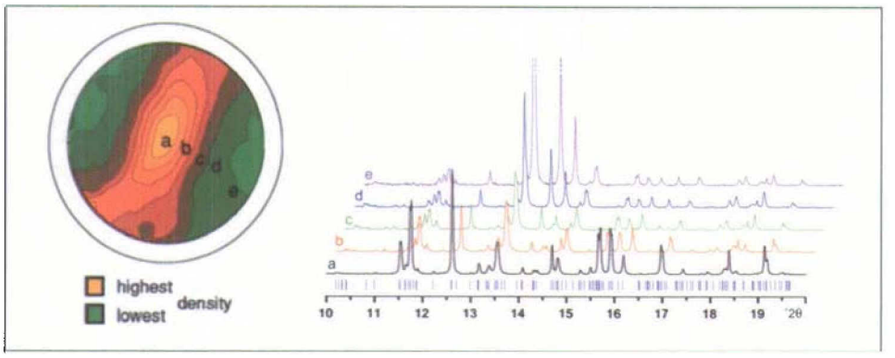

Fig. 8. On the left is the pole figure for the $10\bar{2}$ reflection of the textured UTD-1F sample. The tilt angle χ increases along the radius (0° at the center and 90° at the outermost circle) and the rotation angle ϕ increase counterclockwise around the circle (0° at the right and 180° at the left). On the right are small sections of the five diffraction patterns ($\lambda = 0.99747$ Å) collected at the sample orientations indicated in the pole figure.

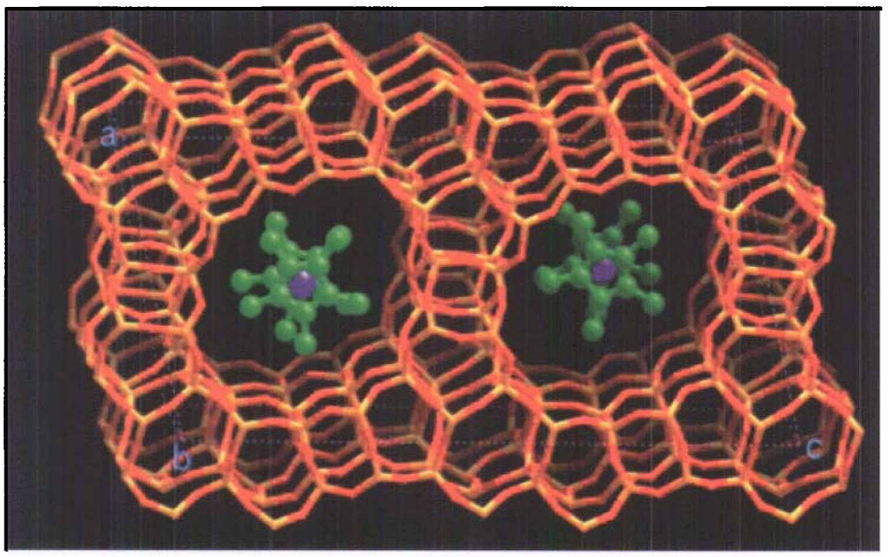

Fig. 9. The structure of UTD-1F in the space group *Pc* showing the framework structure and the ordering of the $Co(Cp^*)_2^+$ complexes in the 14-ring channels. Note that the complexes in the two channels are displaced with respect to one another by 1/2 *b*.

the number of positional parameters (from 207 to 349) was understood to be problematical. Surprisingly, the refinement then proceeded smoothly and eventually converged with $R_F = 0.041$ and $R_{wp} = 0.134$ ($R_{exp} = 0.101$). The weight of the geometric restraints on the atoms of the framework and the Co complex could be reduced to 1.0 (*i.e.* each restraint has the same weight as a single point in the diffraction pattern) and the atomic positions remained stable and chemically sensible. In the final structure, with 117 atoms (32 Si, 64 O, 1 Co and 20 C) in the asymmetric unit, the Co complex is found to be completely ordered in the 14-ring channels (Fig. 9). To the best of our knowledge, this is the most complex structure to have been solved from powder diffraction data using computer methods.

5. Conclusions

Three new approaches to zeolite structure determination from powder diffraction data have been described. Each exploits a different phenomenon: the *focus* approach supplements the diffraction data with well-established chemical information, a structure envelope, which can be used to facilitate structure solution in direct space, is calculated from just a few low-angle reflections (*i.e.* those that are best separated in a powder pattern), and the texture approach uses orientation space to extract more single-crystal-like reflection intensities. Although the *focus* approach is zeolite-specific, the other two are applicable to any class of material. The strengths of these methods are apparent in the examples given. Certainly, the determination of the structure of the high-silica zeolite UTD-1F, with 117 atoms in the asymmetric unit, is a convincing demonstration of the power of powder diffraction techniques in structure analysis.

Acknowledgements

Experimental assistance from the staff of the Swiss-Norwegian Beamlines at the European Synchrotron Radiation Facility in Grenoble is gratefully acknowledged. We also thank Dr. E.J. Creyghton for providing us with the UTD-1F sample, and the Swiss National Science Foundation for continuing support on this project.

Received: March 30. 2001

[1] C. Baerlocher, W.M. Meier, D.H. Olson, 'Atlas of Zeolite Framework Types', Elsevier, Amsterdam, **2001**.
[2] H. Rietveld, *J. Appl. Crystallogr.* **1969**, *2*, 65.
[3] R.B. Von Dreele, *J. Appl. Crystallogr.* **1999**, *32*, 1084.
[4] T. Wessels, C. Baerlocher, L.B. McCusker, E.J. Creyghton, *J. Am. Chem. Soc.* **1999**, *121*, 6242.
[5] G.S. Pawley, *J. Appl. Crystallogr.* **1981**, *14*, 357.
[6] A. Le Bail, H. Duroy, J.L. Fourquet, *Mater. Res. Bull.* **1988**, *23*, 447.
[7] W.I.F. David, K. Shankland, L.B. McCusker, C. Baerlocher, Eds. 'Structure Determination from Powder Diffraction Data', Oxford University Press, in press.
[8] R.W. Grosse-Kunstleve, L.B. McCusker, C. Baerlocher, *J. Appl. Crystallogr.* **1997**, *30*, 985.
[9] P. Wagner, S.I. Zones, M.E. Davis, R.C. Medrud, *Angew. Chem. Int. Ed.* **1999**, *38*, 1269.
[10] R.W. Grosse-Kunstleve, L.B. McCusker, C. Baerlocher, *J. Appl. Crystallogr.* **1999**, *32*, 536.
[11] S. Brenner, L.B. McCusker, C. Baerlocher, *J. Appl. Crystallogr.* **1997**, *30*, 1167.
[12] S. Brenner, 'Structure Envelopes and their Application in Structure Determination from Powder Diffraction Data', ETH-Dissertation Nr. 13280, **1999**; S. Brenner, L.B. McCusker, C. Baerlocher, in preparation.
[13] D. Sayre, *Acta Crystallogr. A* **1952**, *5*, 60; D. Sayre 'Theory and Practice in Direct Methods in Crystallography', Eds. M.F.C. Ladd , R.A. Palmer, Plenum Press, New York, **1980**, pp. 271–286.
[14] G. Bricogne, *Acta Crystallogr. D* **1993**, *49*, 37.
[15] R. Hedel, H.J. Bunge, G. Reck, *Textures Microstruct.* **1997**, *29*, 103.
[16] W. Lasocha, H. Schenk, *J. Appl. Crystallogr.* **1997**, *30*, 561.
[17] R. Cerny, *Mat. Sci. Forum* **1999**, *321–324*, 22.
[18] T. Wessels, C. Baerlocher, L.B. McCusker, *Science* **1999**, *284*, 477.